Thermally conductive polymer composites with hexagonal boron nitride for medical device thermal management

Nu Bich Duyen Do
Department of Microsystems
University of South-Eastern Norway
Borre, Norway
nu.b.do@usn.no

Kristin Imenes *
Department of Microsystems
University of South-Eastern Norway
Borre, Norway
* Correspondence:
Kristin.Imenes@usn.no

Knut E. Aasmundtveit
Department of Microsystems
University of South-Eastern Norway
Borre, Norway
Knut.Aasmundtveit@usn.no

Hoang-Vu Nguyen
Department of Microsystems
University of South-Eastern Norway
Borre, Norway
Hoang.V.Nguyen@usn.no

Erik Andreassen
Sintef Industry
Oslo, Norway
Department of Microsystems
University of South-Eastern Norway
Borre, Norway
Erik.Andreassen@sintef.no

***Abstract*—Polymer composites with hexagonal boron nitride (hBN) have the potential to meet the heat dissipation and electrical insulation requirements of electronic and medical devices. In this study, hBN/polymer composites were fabricated with thermoplastic polyurethane (TPU) and epoxy as matrix materials. Three hBN powder types (BN1, BN2, BN3) with different platelet sizes and degrees of agglomeration were used. BN1 (with average size of 1 µm) and BN2 (with average size of 12 µm) mainly contained hBN platelets, while BN3 (with average size of 20 µm) contained both platelets and agglomerates of platelets. BN2 gave the highest thermal conductivity, while BN1 gave the lowest thermal conductivity.**

Thermal simulations were performed for a medical device with a limit for the maximum surface temperature. For the encapsulation of this device, several material combinations were simulated, using anisotropic thermal conductivity data. This included encapsulations with inner layers of commercial thermally and electrically conductive materials and an outer layer of the best thermally conductive (and electrically insulating) hBN/TPU composite fabricated by the authors.

Keywords—thermally conductive polymer composites, hexagonal boron nitride, thermoplastic polyurethane, epoxy, injection moulding, powder bed fusion, casting, thermal management.

I. INTRODUCTION

For electronic devices, thermal management is vital for ensuring proper operation and preventing failures. In addition to efficient heat dissipation, electrical insulation is required for many applications, such as medical devices. Thermally conducting and electrically insulating polymer-based composites are therefore often used in electronics packaging [1]–[3]. Polymer composites have advantages of low density, low cost, and flexible processing via different techniques, such as injection moulding. Most polymers possess low thermal conductivity (0.1–0.5 W/mK) [4]. Incorporating inorganic fillers into polymer matrix is an effective solution for improving the thermal conductivity, while preserving the electrical insulation [1], [4], [5]. Common inorganic fillers are crystalline ceramic materials, either metal oxides (e.g. alumina (Al_2O_3), quartz (crystalline SiO_2)), or non-oxides (e.g., aluminium nitride (AlN), boron nitride (BN), silicon nitride (Si_3N_4), silicon carbide (SiC)) [1], [4], [5].

Hexagonal boron nitride (hBN) has emerged as a promising filler for polymer composites due to its high intrinsic thermal conductivity, good electrical insulation, high thermal stability, good mechanical properties, and suitability for biomedical applications [6]–[10]. The filler hBN has been studied for enhancing the thermal conductivity of polymer-based composites, see examples in Table 1.

Hexagonal BN consists of B and N atoms arranged in a honeycomb configuration with a layer structure. Within the layers there are strong covalent bonds between B and N atoms, while between the layers there are weak van der Waals forces [6], [7]. The crystal structure of hBN results in platelet-shaped particles. The platelets have high in-plane thermal conductivity of about 300–600 W/mK, whereas the through-plane value is in the range of 2–30 W/mK [3], [6], [7]. Due to the strong B–N bonds, hBN is chemically stable, e.g., towards oxidation. However, this makes the functionalisation of hBN challenging [7].

Due to the hBN platelets' shape and anisotropic thermal conductivity, the orientation of the hBN platelets in the polymer matrix affects the thermal conductivity of the composite [4], [6]. Platelets can be oriented via processing or by using electric or magnetic fields [4], [6], [11]–[13]. Different processing methods have different impacts regarding distributing and orienting the platelets, as well as dispersing agglomerates and stacks of platelets into single platelets.

In scientific studies, thermally conductive polymer composite specimens are commonly fabricated by methods such as injection moulding (IM) and casting [1], [4], [6]. The hBN platelets are reported to be preferentially oriented with the platelet normal in the through-plane (thickness) direction of injection moulded parts, due to the flow in the IM process [4], [6]. Hence, the in-plane conductivity is higher than the through-plane conductivity, as shown in Table 1. In a casting process, composites are produced by mixing fillers into a

Funding: Research Council of Norway (269618 "Mechanical miniaturization in interventional medical instruments"); Norwegian Micro- and Nano-Fabrication Facility (295864 NORFAB III).

Table 1. Some studies of hBN/polymer composites. (wt% = weight percentage, vol% = volume percentage).

Materials	Filler loading (filler size)	Processing method	Thermal conductivity
hBN/epoxy [11]	95 wt%	Compression moulding	21.3 W/m·K (in-plane) 7 W/m·K (through-plane)
hBN/PU [14]	80 vol%	Freeze drying & hot pressing	39 W/m·K (in-plane) 11.5 W/m·K (through-plane)
hBN/polyimide [15]	60 vol%	Spin-cast (film)	17.5 W/m·K (in-plane) 5.4 W/m·K (through-plane)
hBN/epoxy [16]	57 vol% (5–11 μm)	Casting	5.27 W/m·K (through-plane)
hBN/PE [17]	50 vol% (4–5 μm)	Injection moulding	3.66 W/m·K (through-plane)
hBN/PEEK [18]	60 wt% (25–30 μm)	Injection moulding	12.45 W/m·K (in-plane) 2.34 W/m·K (through-plane)
hBN/TPU [19]	50 wt%	Solution mixing & hot pressing	3.06 W/mK (through-plane)
hBN/PA12 [20]	40 wt%	Powder bed fusion	0.55 W/m·K (through-plane, 77% higher than PA12)
hBN/Al_2O_3/PA12 [21]	15 wt% hBN and 35 wt% Al_2O_3	Powder bed fusion	1.05 W/m·K (through-plane, 275% higher than PA12)
hBN/AlN/TPU [22]	15 wt% hBN and 20 wt% AlN	Powder bed fusion	0.9 W/m·K (through-plane, 391% higher than TPU)
hBN/TPU [23]	30 wt%	Fused deposition modeling (material extrusion)	1.51 W/m·K (in-plane) 1.26 W/m·K (through-plane)

resin such as epoxy, followed by pouring or injecting the mixture into a mould for curing. The casting of hBN/polymer composites can result in almost randomly oriented platelets [4], [6], [16].

Powder bed fusion (PBF) is one of the most common 3D printing (additive manufacturing) processes for polymer materials. The feedstock is powder, and thermal energy (e.g., from a laser) selectively fuses regions of a powder bed, layer-by-layer, to fabricate 3D objects [24]. Compared to moulding processes, the principal advantages of PBF and other 3D printing techniques include fast prototyping and geometric freedom. Few polymer types are commercially available for PBF, but the most common are polyamide 12 (PA12) and thermoplastic polyurethane (TPU). There are several articles about polymer PBF with thermally and electrically conductive fillers (e.g., carbon-based fillers such as carbon fibres [25], graphite [26], CNT [27] and graphene [28], or metal fillers such as Cu [29] and Ag [30]). The literature on PBF with thermally conductive and electrically insulating polymer-based composites is sparse, and most studies use PA12 as the polymer matrix [24], [31], [32].

Encapsulation materials of medical devices used in the human body are required to have good heat transfer, electrical insulation, biocompatibility, and in some cases, a 'soft touch' [2], [33]. To achieve a significant increase in thermal conductivity in polymer-based composites, a high loading of inorganic fillers (e.g. hBN) is generally required. However, this normally results in increased hardness [4], [6] and reduced ductility. To compensate for this, a soft polymer can be used as the matrix material. The hBN loading also has a negative effect on the processability via higher viscosity.

Thermally conductive polymer composites can be used for the encapsulation of medical devices such as trans-esophageal echocardiography (TEE) probes. This device uses ultrasound waves to image the heart in 3D from inside the human esophagus. For the patient safety, the encapsulation of the device's scan head is required to provide good heat transfer (the maximum surface temperature of the scan head in contact with human tissue must be below 43 ºC), electromagnetic interference (EMI) shielding, electrical insulation, and biocompatibility.

Thermoplastic polyurethane (TPU) is a soft thermoplastic elastomer, offering high elasticity over a broad temperature range and high wear resistance [24], [32], [34]. It is commonly used for PBF and IM, and its suitability for biomedical applications has recently been highlighted [31]. Therefore, the TPU "Ultrasint TPU 88A" (in the form of powder for PBF) was selected as the matrix for composites processed by PBF and IM in this study.

This study is a continuation of our previous research on the encapsulation of interventional medical devices [33] and thermally conductive polymer composites [35]. This paper adds results for composites with different hBN powder types, and how the hBN platelets' orientation in the injection moulding process can be simulated. Furthermore, thermal simulations for a TEE scan head are performed with various polymer composites, and with anisotropic thermal conductivity, representative of injection moulded polymer composites.

II. Methodology

A. Experiments

Materials

The polymer matrix for injection moulding and powder bed fusion (3D printing) was thermoplastic polyurethane (TPU), in the form of powder, with 88 shore A hardness (Ultrasint TPU 88A, BASF, Germany). The polymer matrix for casting was an epoxy containing 35 wt% unmodified bisphenol-F epoxy resin (Araldite GY 285-1), 35 wt% reactive diluent (Araldite DY 026), 30 wt% amine-based curing agent (Jeffamine D-230 Polyetheramine), from Huntsman. The epoxy system was formulated to have a low viscosity, suitable for preparing composites with high filler loading.

Three hBN powder types (BN1, BN2, BN3) with different platelet sizes and agglomeration degrees were used. BN1 had an average particle size of 1 μm (product no. 255475, Sigma Aldrich, Merck). BN2 and BN3 were supplied by Henze Boron Nitride Products AG, Germany. BN2 (HeBoFill LL-SP 120) [36] and BN3 (HeBoFill CL-ADH 020) [37] had an average particle size of 12 μm and 20 μm, respectively. BN1 and BN2 mainly contained hBN platelets, while BN3 had a partly agglomerated particle structure, claimed to provide good lubricating properties and low viscosity increase [37]. Platelets and spherical agglomerates of hBN are shown in Figure 1.

Specimen preparation by injection moulding, casting, and powder bed fusion

Injection moulded specimens were prepared using a 15 cm^3 micro batch compounder (DSM Midi 2000) followed by injection moulding with a table-top machine (DSM). Moulded

specimens for thermal conductivity measurement were 2 mm thick discs with diameters of 25 mm, see Figure 2. Specimens were prepared with 0, 15, 25, 35, 50 and 65 wt% BN3; 50 wt% BN2; and 50 wt% BN1.

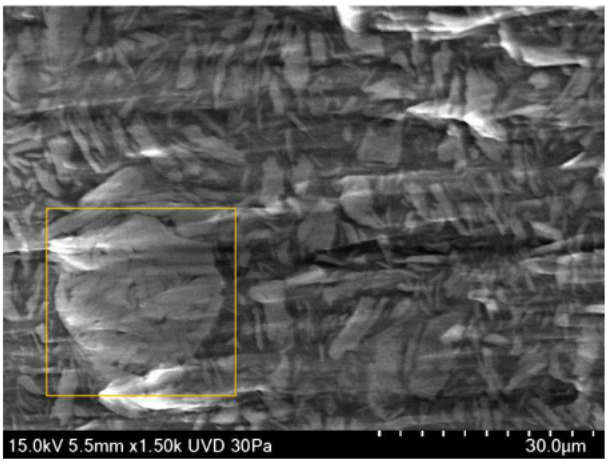

Figure 1: SEM micrograph of ion milled cross-section of the cast specimen with 55 wt% BN3. An agglomerate of hBN platelets is seen inside the yellow square.

Cast epoxy-hBN specimens were prepared by vacuum mixing, followed by casting into a Teflon mould (Figure 2) and then curing at 150 °C for 18 h. The cast specimens (2 mm thick discs) were grinded and polished on both sides. Specimens with 0, 35, 50 and 55 wt% BN3 were cast.

For powder bed fusion (PBF), a tabletop PBF 3D printer (Sharebot SnowWhite) was used to fabricate specimens of a (TPU and hBN) powder mixture. PBF specimen were prepared with 0, 35, 40 wt% BN3; 35 wt% BN2; and 35 wt% BN1.

Thermal conductivity measurements

The thermal conductivity of 2 mm thick specimens was indirectly determined by the non-contact, transient laser flash analysis (LFA) method. Details about the measurements are given in [35].

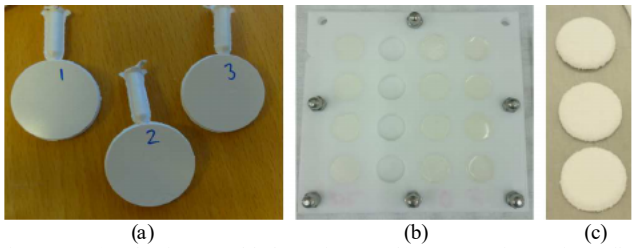

(a) (b) (c)

Figure 2. (a) Injection moulded specimens; (b) cast specimens in Teflon moulds; (c) PBF specimens.

B. Simulation of steady-state heat transfer

A TEE scan head with a two-layer encapsulation was used as a simulation model, which was previously reported in ref. [33], in order to evaluate the thermal performance when the outer layer is made of hBN/polymer composite. Previously, only isotropic thermal conductivity has been considered. However, hBN platelets typically induce anisotropic conductivity (see Table 1). Hence, anisotropic conductivity is included in the present simulation study.

The model represents the test sample used in experiments, see Figure 3. The two-layer encapsulation can be a metallized polymer composite (case 1 in Table 2), or it can consist of two polymer composites (case 2 in Table 2).

The metallized encapsulation (case 1) consists of a metal layer (0.15 mm) deposited on the inner surface of prefabricated polymer composite part (0.9 mm). The metal layer provides heat transfer and EMI shielding, while the outer layer provides electrical insulation, biocompatibility, and some heat transfer.

An encapsulation consisting of two composite layers (case 2) can be fabricated by methods such as two-component injection moulding. Both layers will contribute to the heat transfer. The outer layer should be thermally conductive, but electrically insulating and biocompatible. The inner layer should be thermally and electrically conductive, to take care of both heat transfer and EMI shielding. The thickness limit of the current encapsulation of the TEE scan head is ca. 1 mm. Therefore, the total encapsulation thickness was 1 mm in the simulations.

Table 2: Material data used in the thermal simulations.

Component	**Material**	**Thermal conductivity *k* ($Wm^{-1} K^{-1}$)**
Heat source	Metal ceramic heater [38]	20
Heat sink	Al alloy 6082 [39]	180
Adhesive between heat source and heat sink	Thermally conductive adhesive [40]	1.3
Adhesive between heat sink and encapsulation	Thermally and electrically conductive adhesive [41]	2.5
Coverage of the hole for the electrical wires	Medical silicone	0.2*
Remaining volume inside the sample	Air [42]	k(T) via COMSOL's material library
Case 1: Metallized encapsulation (metallized polymer, or metallized polymer composite)		
Inner layer (0.15 mm)	Electroplated Cu [43]	380
Outer layer (0.9 mm)	Typical polymer material (case 1a)	0.2* (isotropic)
	hBN/TPU, assumed isotropic (case 1b)	2.1 (isotropic)
	hBN/TPU, anisotropic (case 1c)	2.1 (through-plane) ** (this work) 12 (in-plane) ** [18]
Case 2: Encapsulation consisting of two composite layers (total thickness 1.0 mm)		
Inner layer; 0.5 mm (case 2a) or 0.9 mm (case 2b)	Thermally and electrically conductive polymer composite from Celanese	4.5 (through-plane) *** 34 (in-plane) *** [44]
Outer layer; 0.5 mm (case 2a) or 0.1 mm (case 2b)	hBN/TPU (thermally conductive and electrically insulating)	2.1 (through-plane) ** (this work) 12 (in-plane) ** [18]

* Values from references [45], [46].

** The through-plane value (2.1 W/mK) is the highest obtained in our experimental study. The in-plane value (12 W/mK) is estimated based on ref. [18] which studied the anisotropic thermal conductivity of injection moulded hBN/PEEK composites. The highest in-plane and through-plane values in that study were 2 W/mK and 12 W/mK, respectively, for 60 wt% hBN (with size of 25 – 30 µm).

*** Values based on a commercial material (Celanese CoolPoly E5521) [44]. These values seem to be among the highest reported for commercial materials. Other materials were also simulated; one from Avient (with 5.5 W/mK through-plane and 19 W/mK in-plane) and one from Sabic (with 1.5 W/mK through-plane and 18 W/mK in-plane).

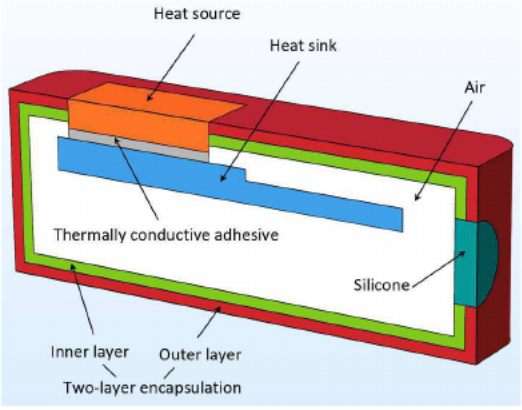

Figure 3: Schematic of cross-section of the test sample (not drawn to scale) used in experiments. See ref. [33] for details.

III. RESULTS AND DISCUSSIONS

A. *Thermal conductivity of hBN/polymer composites*

This section reports the effects of filler loading, filler type and processing method on the thermal conductivity. Figure 4 shows the thermal conductivity of hBN/polymer composites fabricated by injection moulding (IM), casting (C) and powder bed fusion (PBF) as a function of hBN loading. The highest conductivity (2.1 W/mK) was measured for an injection moulded specimen with the highest hBN loading in this study (65 wt% BN3). This conductivity is almost 900% higher than that of the pure TPU (injection moulded reference). For the cast composites, a 1313% higher conductivity was obtained with 55 wt% BN3. For a given hBN loading, the cast composites had the highest conductivity and the highest increase relative to the unfilled material. Among the PBF composites, the specimen with 40 wt% BN3, processed with the highest laser energy density, had the highest conductivity, which was 460% higher than that of the pure TPU (fabricated by PBF).

Figure 4 also shows that for IM composites with 50 wt% hBN, BN2 and BN1 gave the highest and lowest thermal conductivity, respectively. The same trend was observed for the PBF composites, although the effect was weaker.

With the same hBN loading, BN2 results in higher conductivity than BN3. Although some agglomerates in BN3 are broken up during processing, the lower conductivity with BN3 is probably due to platelets being less dispersed. Powders with hBN agglomerates, such as BN3, are claimed to have more isotropic properties and easier processing due to a lower viscosity from spherical fillers [4].

BN1 gives lower thermal conductivity than the two other powders at the same filler loading. This effect is observed for both IM and PBF specimen. The smaller platelets in BN1 gives a larger total surface area. This will reduce the conductivity of the composite if the matrix-filler interfacial thermal resistance is high [47]. The weak bonding between the polymer matrix and the hBN surface probably lead to high interfacial thermal resistance [48].

The surface of the hBN particles can be modified chemically in order to improve the dispersion of hBN particles and achieve a stronger hBN/polymer interface, thereby improving the thermal conductivity and the mechanical properties [7], [10], [49]–[51]. However, the chemical inertness and oxidation resistance of hBN make the functionalisation of hBN challenging.

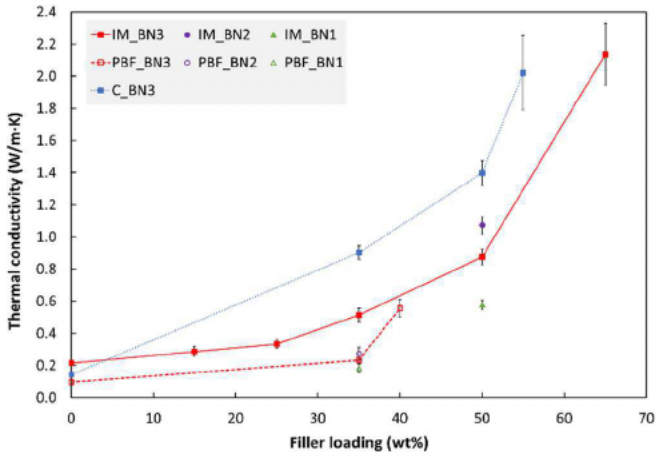

Figure 4. Thermal conductivity (at 30 ºC) of composites fabricated by injection moulding ("IM"), powder bed fusion ("PBF") and casting ("C") as a function of hBN loading. The PBF specimen with 40 wt% BN3 was processed with a higher laser energy density than the other PBF specimens in this figure.

B. *Anisotropy of thermal conductivity*

The injection moulded composites in our study have lower conductivity than the cast composites. This is due to the preferred in-plane orientation of the hBN platelets in the former case, as shown by the XRD data in ref. [35]. Casting only resulted in a low preferred orientation, and powder bed fusion resulted in an almost random orientation.

In our previous work [35] we showed that injection moulding induces a preferred orientation of the platelets, with the platelet normal along the thickness direction of the specimens. The orientation varied through the thickness of the moulded specimens, and it increased with increasing hBN loading. Filler orientation by injection moulding was also reported by Grundler et al. [52] for their polymer composites with graphite flakes.

Numerical simulations of the injection moulding process were performed to illustrate how the platelets achieve their preferred orientation through the thickness of the injection moulded discs. The results agreed with the $\langle\cos^2\theta\rangle$ values from the XRD measurements. The platelets have in-plane alignment (with high $\langle\cos^2\theta\rangle$) in the 'shell' near the surface of the injection moulded disc, and less preferred alignment (with lower $\langle\cos^2\theta\rangle$) in the core of the disc, see Figure 5.

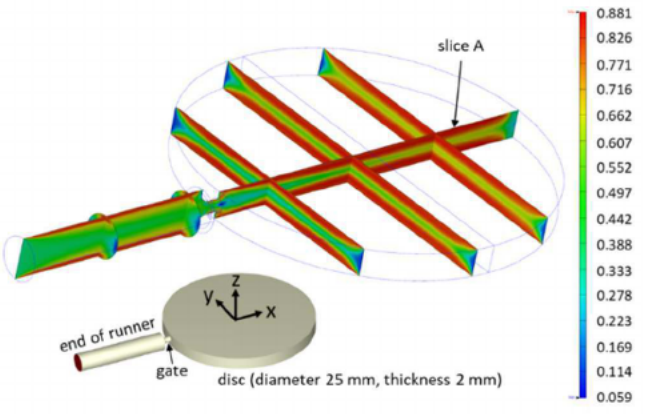

Figure 5: Simulated platelet orientation ($\langle\cos^2\theta\rangle$) in an injection moulded 2 mm thick disc. The orientation data are shown in slices through the thickness of the disc, including gate and part of the runner.

C. *Comparison with published thermal conductivity values*

The thermal conductivity of our composites (hBN/TPU and hBN/epoxy) were compared with some commercially available polymer composites (Table 3) and published values for similar composites (Table 1 and Figure 6). However, such comparisons are challenging, due to differences in mixing/processing method, hBN loading, hBN particle size and matrix material.

The highest through-plane thermal conductivity of our hBN/TPU composites (2.1 W/mK) is higher than that of most commercial thermally conductive and electrically insulating materials, e.g. from Sabic, Covestro, Celanese and Kraiburg (Table 3). However, the commercial materials seem to have better mechanical properties.

Table 3: Through-plane thermal conductivity of some commercially available polymers, that are thermally conductive and electrically insulating and suitable for injection moulding.

Supplier – Materials	Through-plane thermal conductivity (W/mK)
Sabic – LNP Konduit Compounds [53] (with PA6, PPS or PC matrix)	0.6 – 1.5
Covestro - Makrolon TC [54] (with PC matrix)	0.2 – 0.3
Celanese – Coolpoly D Series [44] (with PP, PA6, PPS, LCP, or TPE matrix)	0.6 – 1.9
Kraiburg – Thermoplast K [55] (HTC1500/117, with TPE matrix)	1.5
TCPoly - Ice9 Flex [56] (TPE with two filler types)	2
Our hBN/TPU composites (65 wt% hBN)	2.1

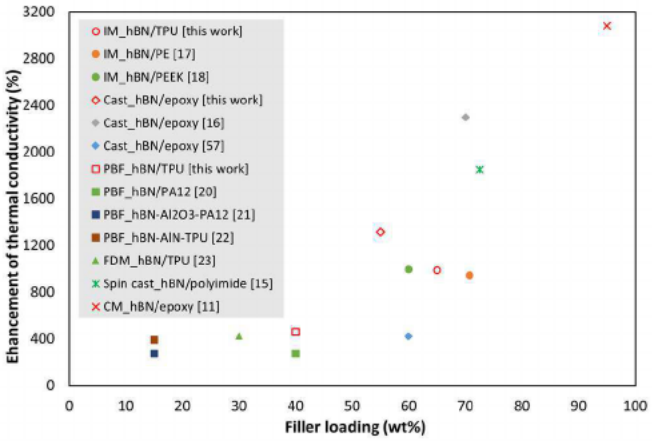

Figure 6: Comparison of the thermal conductivity enhancement (%) for the hBN/polymer composites prepared with different hBN loading (wt%) and processing methods [11], [15]–[18], [20]–[23], [57]. Abbreviations of processing methods in the legend: injection molding (IM), powder bed fusion (PBF), fused deposition modeling (FDM), compression molding (CM).

D. *Using thermally conductive composites for the thermal management of medical devices – A simulation study*

This section presents thermal simulations (steady-state heat transfer) for a TEE scan head. Cases and material data are given in Table 2. The scan head encapsulation must fulfil the requirement that the maximum surface temperature (T_{max}) of the scan head (in contact with human tissue) must be below 43 ºC. T_{max} occurs at the surface of the heat source (which is not encapsulated). In most simulations the heat source power was 0.5 W (if nothing else is stated). In some cases, the power was varied to find the value corresponding to T_{max} = 43 °C.

Metallized encapsulation (case 1a-1c)

In our previous study [33], an isotropic metallized polymer encapsulation (case 1a in Table 2) was simulated. For a power of ca 0.5 W, T_{max} reached the limit of 43 °C. If the polymer is replaced by our composite and isotropy is assumed (case 1b, Figure 7a), T_{max} is reduced to 42.2 °C for the same power (0.5 W). T_{max} = 43 °C is reached for a power of 0.59 W. With the anisotropic material model (case 1c, Figure 7b), T_{max} is reduced to 42.1 °C for the same power (0.5 W). The anisotropic material provides better heat transfer, due to its higher in-plane conductivity.

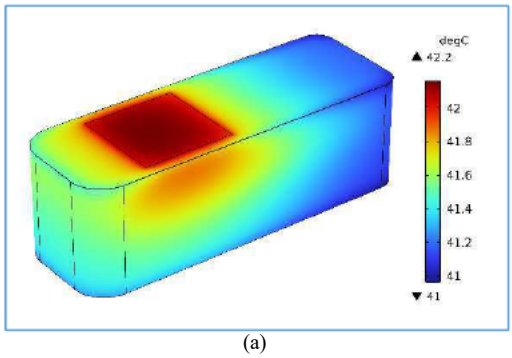

(a)

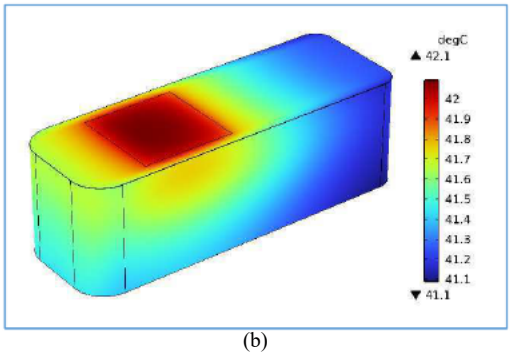

(b)

Figure 7: Simulated surface temperature of the TEE scan head with power 0.5 W. (a) Case 1b in Table 2. (b) Case 1c in Table 2.

Encapsulation consisting of two polymer composite layers (case 2a and 2b)

Two cases of two-layer polymer composite encapsulations were simulated (case 2a and 2b in Table 2). Both layers have fillers that increase the thermal conductivity. The inner layer is electrically conductive, while the outer layer is electrically insulating.

Such encapsulations perform similar to the metallized encapsulations (Figure 8 vs. Figure 7). With our hBN/TPU composite in the outer layer and the Celanese composite in the inner layer, the limit T_{max} = 43 °C is reached for a power level in the range 0.55-0.60 W.

Commercial polymer composites have different conductivities and degrees of thermal anisotropy. To investigate the overall effect on the surface temperature, simulations were performed with a range of different in-plane and through-plane thermal conductivities for the inner layer, see Figure 9. First, we notice that the difference in T_{max} between the four inner layer materials (white symbols in the figure) is small (T_{max} values within 1 °C, and below the 43 °C limit). The Celanese material (triangle) is the best, with the lowest T_{max} for both cases (0.5/0.5mm and 0.9/0.1mm).

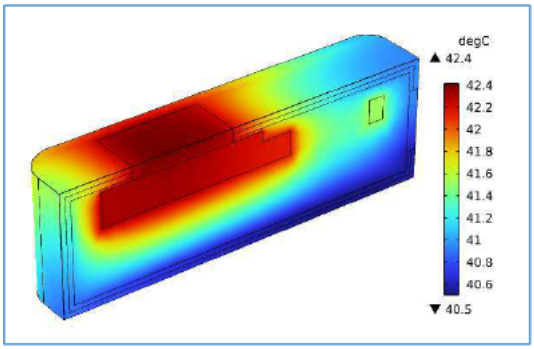

(a)

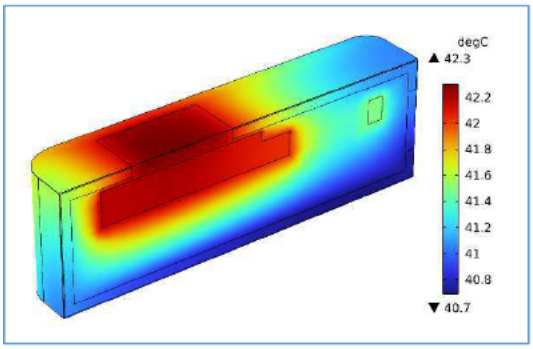

(b)

Figure 8: Heat transfer simulation of the TEE scan head (half model) with power 0.5 W. (a) Case 2a (0.5/0.5 mm thickness combination). (b) Case 2b (0.9/0.1 mm thickness combination).

For these four materials, the T_{max} values of the 0.9/0.1mm case and the 0.5/0.5mm case are quite similar. The 0.9/0.1mm case gives slightly lower T_{max} values for the best two materials (triangle and star symbols). When using our hBN/TPU material (square) in both layers of the encapsulation, there is obviously no difference between the two cases.

The difference in T_{max} between the two cases increases with decreasing conductivity values, since the 0.9 mm thick inner layer then gives a larger T_{max}, due to the insulating effect. For low conductivity values (e.g. $k_{through\text{-}plane} < 1$ W/mK), T_{max} is more sensitive to through-plane conductivity than to in-plane conductivity.

The minimum surface temperature T_{min} was also evaluated by simulations. For the 0.9/0.1mm case with low inner layer conductivities (< 0.5 W/mK), T_{min} is within 1 °C of the surrounding temperature (37 °C) due to low heat transfer to the coldest spot. T_{min} is more sensitive to $k_{in\text{-}plane}$ than to $k_{through\text{-}plane}$, as $k_{in\text{-}plane}$ contributes more to transferring heat to the coldest spot on the scan head surface.

The temperature difference ($\Delta T = T_{max} - T_{min}$) decreases with increasing conductivity values, in particular with increasing in-plane values, as more heat is then transferred to the coldest spot on the scan head surface. The material which gives the lowest T_{max} value also gives the lowest ΔT, since distributing heat over the surface lowers T_{max}. With the two best materials, (triangle and star symbols), ΔT is lower for the 0.9/0.1mm case than for the 0.5/0.5mm case.

In future studies, the local platelet orientation induced in the injection moulding process can be simulated (as in Figure 5). From this, the local anisotropic thermal conductivity can be calculated with an appropriate model (some discussed in our previous study [35]). Finally, a thermal simulation can be performed, using the local anisotropic thermal conductivity as material input.

From a heat transfer point of view, the metallized encapsulation and the two-layer composite encapsulation studied in this paper can provide adequate thermal dissipation for the TEE scan head when the power is below 0.6 W. However, the EMI shielding of such encapsulations should be evaluated by experiments.

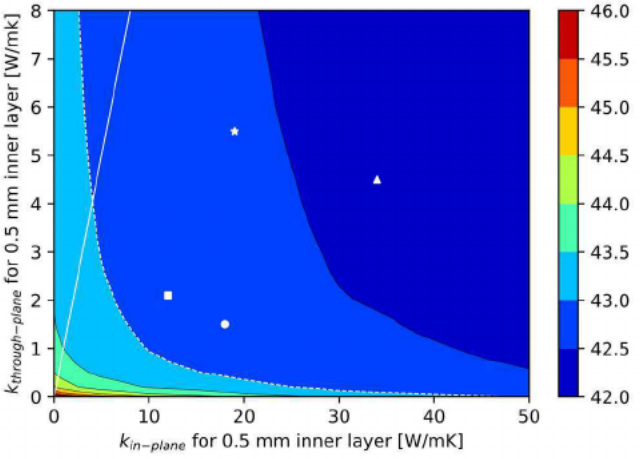

(a)

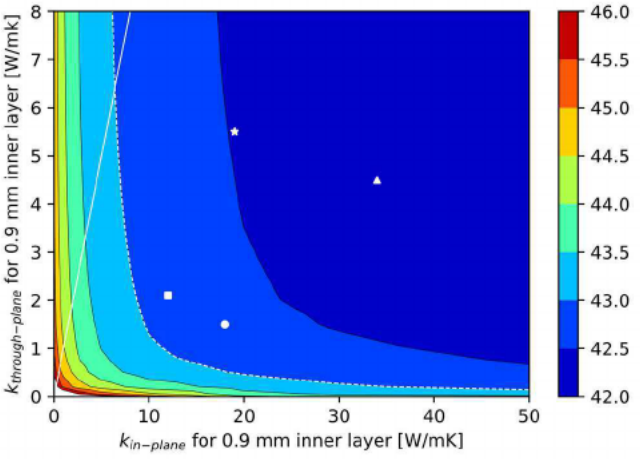

(b)

Figure 9: Contour plots of T_{max} vs. in-plane and through-plane thermal conductivity for the inner layer (case 2). The power is 0.5 W. The white dashed line represents the limit T_{max} = 43 °C, and the white solid line represents isotropic materials. The white symbols represent the four anisotropic materials in Table 2, case 2: The triangle, star and circle represent the materials from Celanese, Avient and Sabic, while the square is the best hBN/TPU composite in this study. (a) Case 2a (0.5/0.5 mm thickness combination). (b) Case 2b (0.9/0.1 mm thickness combination). In this plot, T_{max} values above 46 °C (for low conductivity values) are blank (white).

IV. Conclusions

This study has provided new insights on the effect of hBN powder type on the thermal conductivity of hBN/polymer composites. With the three powder types in this study, both the average particle size and the degree of agglomeration affect the conductivity. The conductivity of the composite is lowest for the smallest platelets. This is probably due to these giving the largest platelet-polymer interface area in combination with high interfacial thermal resistance. Powders with some platelet agglomerates seem to give lower conductivity than powders with only "free"

platelets. The latter result in better dispersed platelets, which are more effective in transferring heat.

The highest through-plane thermal conductivity of the hBN/polymer composites obtained in this study was 2.1 W/mK. The applicability of hBN/polymer composites in a two-layer encapsulation of a TEE scan head was evaluated by thermal simulations. The maximum surface temperature of this scan head must be below 43 °C. A hBN/polymer composite can be used in a metallized encapsulation (with 0.15 mm of Cu and 0.9 mm of hBN/TPU), or in a 1.0 mm thick encapsulation consisting of two layers (an outer layer of hBN/TPU and an inner layer of a commercial thermally and electrically conductive polymer composite). Such encapsulations provide the TEE scan head with adequate heat transfer for power levels up to about 0.6 W.

Finally, we have demonstrated how thermal simulations with anisotropic material data can be used to evaluate and compare anisotropic materials.

ACKNOWLEDGMENT

The authors gratefully acknowledge Paul McMahon at SINTEF Industry; Jeyanthinath Mayandi at University of Oslo; Erik Kalland at Conpart AS; and Zekija Ramic, Svein Mindrebøe, Tayyib Muhammad, Chaoqun Cheng at University of South-Eastern Norway for their enthusiastic assistance with laboratory work. We sincerely thank Terje Finstad at University of Oslo and Helge Kristiansen at Conpart AS for valuable discussions.

REFERENCES

[1] R. Tummala, *Fundamentals of Microsystems Packaging*. McGraw-Hill Education, 2001. [Online]. Available: https://books.google.no/books?id=nf1vwR9VYGEC

[2] R. Bahru, A. A. Hamzah, and M. A. Mohamed, "Thermal management of wearable and implantable electronic healthcare devices: Perspective and measurement approach," *Int. J. Energy Res.*, 2020, doi: 10.1002/er.6031.

[3] C. Yuan, B. Duan, L. Li, B. Xie, M. Huang, and X. Luo, "Thermal Conductivity of Polymer-Based Composites with Magnetic Aligned Hexagonal Boron Nitride Platelets," *ACS Appl. Mater. Interfaces*, vol. 7, no. 23, pp. 13000–13006, 2015, doi: 10.1021/acsami.5b03007.

[4] H. Chen, V. V. Ginzburg, J. Yang, Y. Yang, W. Liu, Y. Huang, L. Du, and B. Chen, "Thermal conductivity of polymer-based composites: Fundamentals and applications," *Prog. Polym. Sci.*, vol. 59, pp. 41–85, 2016, doi: 10.1016/j.progpolymsci.2016.03.001.

[5] D. Li, D. Zeng, Q. Chen, M. Wei, L. Song, C. Xiao, and D. Pan, "Effect of different size complex fillers on thermal conductivity of PA6 thermal composites," *Plast. Rubber Compos.*, vol. 48, no. 8, pp. 347–355, Sep. 2019, doi: 10.1080/14658011.2019.1626596.

[6] C. Yu, J. Zhang, W. Tian, X. Fan, and Y. Yao, "Polymer composites based on hexagonal boron nitride and their application in thermally conductive composites," *RSC Adv.*, vol. 8, no. 39, pp. 21948–21967, 2018, doi: 10.1039/C8RA02685H.

[7] Z. Zheng, M. Cox, and B. Li, "Surface modification of hexagonal boron nitride nanomaterials: a review," *J. Mater. Sci.*, vol. 53, no. 1, pp. 66–99, Jan. 2018, doi: 10.1007/s10853-017-1472-0.

[8] Y. Zhang, W. Gao, Y. Li, D. Zhao, and H. Yin, "Hybrid fillers of hexagonal and cubic boron nitride in epoxy composites for thermal management applications," *RSC Adv.*, 2019, doi: 10.1039/c9ra00282k.

[9] A. Merlo, V. R. S. S. Mokkapati, S. Pandit, and I. Mijakovic, "Boron nitride nanomaterials: Biocompatibility and bio-applications," *Biomater. Sci.*, 2018, doi: 10.1039/c8bm00516h.

[10] G. Ciofani, G. G. Genchi, I. Liakos, A. Athanassiou, D. Dinucci, F. Chiellini, and V. Mattoli, "A simple approach to covalent functionalization of boron nitride nanotubes," *J. Colloid Interface Sci.*, vol. 374, no. 1, pp. 308–314, May 2012, doi: 10.1016/j.jcis.2012.01.049.

[11] Z. Zhu, P. Wang, P. Lv, T. Xu, J. Zheng, C. Ma, K. Yu, W. Feng, W. Wei, and L. Chen, "Densely packed polymer/boron nitride composite for superior anisotropic thermal conductivity," *Polym. Compos.*, vol. 39, no. S3, pp. E1653–E1658, Jun. 2018, doi: 10.1002/pc.24615.

[12] Y. Xue, X. Li, H. Wang, F. Zhao, D. Zhang, and Y. Chen, "Improvement in thermal conductivity of through-plane aligned boron nitride/silicone rubber composites," *Mater. Des.*, vol. 165, pp. 107580–107580, 2019, doi: 10.1016/j.matdes.2018.107580.

[13] Z. Lin, Y. Liu, S. Raghavan, K. S. Moon, S. K. Sitaraman, and C. P. Wong, "Magnetic alignment of hexagonal boron nitride platelets in polymer matrix: Toward high performance anisotropic polymer composites for electronic encapsulation," *ACS Appl. Mater. Interfaces*, vol. 5, no. 15, pp. 7633–7640, 2013, doi: 10.1021/am401939z.

[14] N. Zhao, J. Li, W. Wang, W. Gao, and H. Bai, "Isotropically Ultrahigh Thermal Conductive Polymer Composites by Assembling Anisotropic Boron Nitride Nanosheets into a Biaxially Oriented Network," *ACS Nano*, vol. 16, no. 11, pp. 18959–18967, Nov. 2022, doi: 10.1021/acsnano.2c07862.

[15] M. Tanimoto, T. Yamagata, K. Miyata, and S. Ando, "Anisotropic thermal diffusivity of hexagonal boron nitride-filled polyimide films: Effects of filler particle size, aggregation, orientation, and polymer chain rigidity," *ACS Appl. Mater. Interfaces*, vol. 5, no. 10, pp. 4374–4382, 2013, doi: 10.1021/am400615z.

[16] Y. Xu and D. D. L. Chung, "Increasing the thermal conductivity of boron nitride and aluminum nitride particle epoxy-matrix composites by particle surface treatments," *Compos. Interfaces*, vol. 7, no. 4, pp. 243–256, Jan. 2000, doi: 10.1163/156855400750244969.

[17] G.-W. Lee, M. Park, J. Kim, J. I. Lee, and H. G. Yoon, "Enhanced thermal conductivity of polymer composites filled with hybrid filler," *Compos. Part Appl. Sci. Manuf.*, vol. 37, no. 5, pp. 727–734, May 2006, doi: 10.1016/j.compositesa.2005.07.006.

[18] S. Gul, S. Arican, M. Cansever, B. Beylergil, M. Yildiz, and B. Saner Okan, "Design of Highly Thermally Conductive Hexagonal Boron Nitride-Reinforced PEEK Composites with Tailored Heat Conduction Through-Plane and Rheological Behaviors by a Scalable Extrusion," *ACS Appl. Polym. Mater.*, vol. 5, no. 1, pp. 329–341, Jan. 2023, doi: 10.1021/acsapm.2c01534.

[19] T. Fei, Y. Li, B. Liu, and C. Xia, "Flexible polyurethane/boron nitride composites with enhanced thermal conductivity," *High Perform. Polym.*, vol. 32, no. 3, pp. 324–333, Apr. 2020, doi: 10.1177/0954008319862044.

[20] L. Yang, L. Wang, and Y. Chen, "Solid-state shear milling method to prepare PA12/boron nitride thermal conductive composite powders and their selective laser sintering 3D-printing," *J. Appl. Polym. Sci.*, vol. 137, no. 23, pp. 1–13, 2020, doi: 10.1002/app.48766.

[21] Y. Yuan, W. Wu, H. Hu, D. Liu, H. Shen, and Z. Wang, "The combination of Al 2 O 3 and BN for enhancing the thermal conductivity of PA12 composites prepared by selective laser sintering," *RSC Adv.*, vol. 11, no. 4, pp. 1984–1991, 2021, doi: 10.1039/D0RA09775F.

[22] X. Zhang, W. Wu, T. Zhao, and J. Li, "The combination of AlN and h-BN for enhancing the thermal conductivity of thermoplastic polyurethane composites prepared by selective laser sintering," *J. Appl. Polym. Sci.*, Aug. 2022, doi: 10.1002/app.53051.

[23] J. Gao, M. Hao, Y. Wang, X. Kong, B. Yang, R. Wang, Y. Lu, L. Zhang, M. Gong, L. Zhang, D. Wang, and X. Lin, "3D printing boron nitride nanosheets filled thermoplastic polyurethane composites with enhanced mechanical and thermal conductive properties," *Addit. Manuf.*, vol. 56, pp. 102897–102897, Aug. 2022, doi: 10.1016/j.addma.2022.102897.

[24] S. C. Ligon, R. Liska, J. Stampfl, M. Gurr, and R. Mülhaupt, "Polymers for 3D Printing and Customized Additive Manufacturing," *Chem. Rev.*, vol. 117, no. 15, pp. 10212–10290, 2017, doi: 10.1021/acs.chemrev.7b00074.

[25] F. Sillani, F. de Gasparo, M. Schmid, and K. Wegener, "Influence of packing density and fillers on thermal conductivity of polymer powders for additive manufacturing," *Int. J. Adv. Manuf. Technol.*, vol. 117, no. 7–8, pp. 2049–2058, Dec. 2021, doi: 10.1007/s00170-021-07117-z.

[26] F. Lupone, E. Padovano, O. Ostrovskaya, A. Russo, and C. Badini, "Innovative approach to the development of conductive hybrid composites for Selective Laser Sintering," *Compos. Part Appl. Sci.*

Manuf., vol. 147, pp. 106429–106429, Aug. 2021, doi: 10.1016/j.compositesa.2021.106429.

[27] S. Yuan, Y. Zheng, C. K. Chua, Q. Yan, and K. Zhou, "Electrical and thermal conductivities of MWCNT/polymer composites fabricated by selective laser sintering," *Compos. Part Appl. Sci. Manuf.*, vol. 105, pp. 203–213, Feb. 2018, doi: 10.1016/j.compositesa.2017.11.007.

[28] A. Ronca, G. Rollo, P. Cerruti, G. Fei, X. Gan, G. Buonocore, M. Lavorgna, H. Xia, C. Silvestre, and L. Ambrosio, "Selective Laser Sintering Fabricated Thermoplastic Polyurethane/Graphene Cellular Structures with Tailorable Properties and High Strain Sensitivity," *Appl. Sci.*, vol. 9, no. 5, pp. 864–864, Feb. 2019, doi: 10.3390/app9050864.

[29] L. Lanzl, K. Wudy, S. Greiner, and D. Drummer, "Selective laser sintering of copper filled polyamide 12: Characterization of powder properties and process behavior," *Polym. Compos.*, vol. 40, no. 5, pp. 1801–1809, May 2019, doi: 10.1002/pc.24940.

[30] P. Gruber, G. Ziółkowski, M. Olejarczyk, E. Grochowska, V. Hoppe, P. Szymczyk-Ziółkowska, and T. Kurzynowski, "Influence of bioactive metal fillers on microstructural homogeneity of PA12 composites produced by polymer Laser Sintering," *Arch. Civ. Mech. Eng.*, vol. 22, no. 3, pp. 117–117, Jul. 2022, doi: 10.1007/s43452-022-00442-4.

[31] Shangqin Yuan, "Development and optimization of selective laser sintered-composites and structures for functional applications," 2018. doi: 10.32657/10356/73195.

[32] S. Yuan, F. Shen, C. K. Chua, and K. Zhou, "Polymeric composites for powder-based additive manufacturing: Materials and applications," *Prog. Polym. Sci.*, vol. 91, pp. 141–168, Apr. 2019, doi: 10.1016/j.progpolymsci.2018.11.001.

[33] N. B. D. Do, E. Andreassen, S. Edwardsen, A. Lifjeld, K. E. Aasmundtveit, H.-V. Nguyen, and K. Imenes, "Thermal management of an interventional medical device with double layer encapsulation," *Exp. Heat Transf.*, pp. 1–18, Jul. 2021, doi: 10.1080/08916152.2021.1946208.

[34] A. Frick and A. Rochman, "Characterization of TPU-elastomers by thermal analysis (DSC)," *Polym. Test.*, vol. 23, no. 4, pp. 413–417, Jun. 2004, doi: 10.1016/j.polymertesting.2003.09.013.

[35] N. B. D. Do, K. Imenes, K. E. Aasmundtveit, H.-V. Nguyen, and E. Andreassen, "Thermal Conductivity and Mechanical Properties of Polymer Composites with Hexagonal Boron Nitride—A Comparison of Three Processing Methods: Injection Moulding, Powder Bed Fusion and Casting," *Polymers*, vol. 15, no. 6, p. 1552, Mar. 2023, doi: 10.3390/polym15061552.

[36] Henze Boron Nitride Products AG, "HeBoFill ® LL-SP 120," *Tech. Datasheet*, pp. 8374–8374, 2020.

[37] Henze Boron Nitride Products AG, "HeBoFill ® CL-ADH 020," *Tech. Datasheet*, pp. 49–50, 2020.

[38] Heat Scientific, "Heat Scientific MCH Metal Ceramic Heater," *HS-PS101012Y Datasheet*, 2018.

[39] Aalco, "Aluminium alloy 6082," *Tech. Datasheet*, 2019.

[40] Epoxy Technology, "EPO-TEK T7109-19," *Tech. Datasheet*, 2019.

[41] Epoxy Technology, "EPO-TEK EJ2189-LV," *Tech. Datasheet*, 2017.

[42] COMSOL Multiphysics v. 5.3a, "COMSOL Material Library," *COMSOL AB Swden*, 2018.

[43] K. Jagannadham, "Thermal conductivity of copper-graphene composite films synthesized by electrochemical deposition with exfoliated graphene platelets," *Metall. Mater. Trans. B Process Metall. Mater. Process. Sci.*, 2012, doi: 10.1007/s11663-011-9597-z.

[44] Celanese, "Celanese Thermally conductive plastics CoolPoly TCP." Celanese corporation, 2023. [Online]. Available: https://www.celanese.com/products/coolpoly-thermal-conductivity-plastics/

[45] G. Wypych, *Handbook of Polymers: Second Edition*. 2016. doi: 10.1016/C2015-0-01462-9.

[46] A. J. T. Teo, A. Mishra, I. Park, Y. J. Kim, W. T. Park, and Y. J. Yoon, "Polymeric Biomaterials for Medical Implants and Devices," *ACS Biomaterials Science and Engineering*. 2016. doi: 10.1021/acsbiomaterials.5b00429.

[47] J. Ordonez-Miranda and J. J. Alvarado-Gil, "Thermal conductivity of nanocomposites with high volume fractions of particles," *Compos. Sci. Technol.*, vol. 72, no. 7, pp. 853–857, Apr. 2012, doi: 10.1016/j.compscitech.2012.02.016.

[48] K. Pietrak and T. Wiśniewski, "A review of models for effective thermal conductivity of composite materials," *J. Power Technol.*, vol. [Online] 95:1, 2014.

[49] S. Daneshmehr, F. Román, and J. M. Hutchinson, "The surface modification of boron nitride particles," *J. Therm. Anal. Calorim.*, 2019, doi: 10.1007/s10973-019-09160-1.

[50] Z. Cui, A. J. Oyer, A. J. Glover, H. C. Schniepp, and D. H. Adamson, "Large scale thermal exfoliation and functionalization of boron nitride," *Small*, 2014, doi: 10.1002/smll.201303236.

[51] S. Ryu, K. Kim, and J. Kim, "Silane surface treatment of boron nitride to improve the thermal conductivity of polyethylene naphthalate requiring high temperature molding," *Polym. Compos.*, vol. 39, no. S3, pp. E1692–E1700, Jun. 2018, doi: 10.1002/pc.24680.

[52] M. Grundler, T. Derieth, and A. Heinzel, "Polymer compounds with high thermal conductivity," presented at the PROCEEDINGS OF THE REGIONAL CONFERENCE GRAZ 2015 – POLYMER PROCESSING SOCIETY PPS: Conference Papers, Graz, Austria, 2016, p. 030015. doi: 10.1063/1.4965485.

[53] Sabic, "Rethinking your heat sink materials." Sabic, 2020. [Online]. Available: https://www.sabic.com/en/industries/electrical-and-electronics/lighting/thermal-conductive

[54] Covestro Deutschland AG - Engineering Plastics, "Whitepaper 'Power-Tools mit maximaler Leistung und Lebensdauer.'" Covestro, 2022. [Online]. Available: https://solutions.covestro.com/en/highlights/articles/theme/product-technology/makrolon-tc-thermal-conductive-plastics-next-generation-heat-management

[55] Kraiburg, "Technical datasheet - Kraiburg THERMOLAST K (HTC1500/117)." Kraiturg TPE, 2023. [Online]. Available: https://www.kraiburg-tpe.com/en/thermolast-k

[56] TCPoly, "Technical datasheet - Ice9 Flex (Thermally conductive, electrically non-conducting plastic TC-TPE1-145-000)." TCPoly, 2019. [Online]. Available: https://tcpoly.com/purchase-ice9-materials/

[57] J. Gu, Q. Zhang, J. Dang, and C. Xie, "Thermal conductivity epoxy resin composites filled with boron nitride: THERMAL CONDUCTIVITY EPOXY RESIN COMPOSITES," *Polym. Adv. Technol.*, vol. 23, no. 6, pp. 1025–1028, Jun. 2012, doi: 10.1002/pat.2063.